KERNFORSCHUNGSZENTRUM

KARLSRUHE

Thermodynamic State, Specific Heat, and Enthalpy Function of Saturated UO$_2$ Vapor between 3000 K and 5000 K

H. U. Karow

KERNFORSCHUNGSZENTRUM KARLSRUHE

KFK 2390

Institut für Neutronenphysik und Reaktortechnik
Projekt Schneller Brüter

Thermodynamic State, Specific Heat, and Enthalpy
Function of Saturated UO_2 Vapor between 3000 K
and 5000 K

H. U. Karow
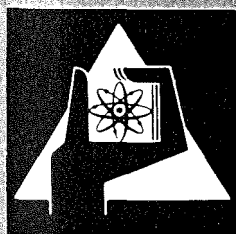
Gesellschaft für Kernforschung mbH., Karlsruhe

Thermodynamic State, Specific Heat, and Enthalpy Function

of Saturated UO_2 Vapor between 3000 K and 5000 K

Abstract

Reactor safety analysis requires knowledge of the thermophysical
properties of molten oxide fuel and of the thermal equation-of-
state of oxide fuel in thermodynamic liquid-vapor equilibrium far
above 3000 K. In this context, the thermodynamic state of satu-
rated UO_2 fuel vapor, its internal energy $U(T)$, specific heats
$C_v(T)$ and $C_p(T)$, and enthalpy functions $H^O(T)$ and $H^O(T)-H^O_o$ have
been determined by means of statistical mechanics in the tempera-
ture range 3000 K ... 5000 K. The discussion of the thermodynamic
state includes the evaluation of the plasma state and its contri-
bution to the caloric variables-of-state of saturated oxide fuel
vapor. Because of the extremely high ion and electron density due
to thermal ionization, the ionized component of the fuel vapor
does no more represent a perfect kinetic plasma - different from
the nonionized neutral vapor component with perfect gas kinetic
behavior up to about 5000 K. At temperatures around 5000 K, UO_2
vapor reaches the collective plasma state and becomes increasingly
"metallic". - Moreover, the nonuniform molecular equilibrium
composition of UO_2 vapor has been taken into account in calcu-
lating its caloric functions-of-state, based on the equilibrium
compositions of Breitung's oxygen potential approach. The contri-
bution to specific heat and enthalpy of thermally excited electronic
states of the vapor molecules has been derived by means of a
Rydberg orbital model of the UO_2 molecule.

The resulting enthalpy functions and specific heats for saturated
UO_2 vapor of equilibrium composition and that for pure UO_2 gas are
compared with the enthalpy and specific heat data of gaseous UO_2
at lower temperatures known from literature. Tentatively also
experimental enthalpy data of the condensed phases of UO_2 have
been converted into the vapor phase using the Clausius-Clapeyron
equation. However, the correlation based on the Clausius-Clapeyron
equation turns out to fail because this equation is not applicable
to the chemically reactive oxide fuel system.

Thermodynamischer Zustand, spezifische Wärme und Enthalpie

von gesättigtem UO_2-Dampf zwischen 3000 K und 5000 K

Zusammenfassung

Die Reaktorsicherheitsanalyse fordert die Kenntnis der thermo-physikalischen Eigenschaften von geschmolzenem Oxidbrennstoff sowie seiner thermischen Zustandsgleichung für das thermodyna-mische Flüssig-Dampfgleichgewicht. Im Zusammenhang hiermit behandelt der vorliegende Bericht den thermodynamischen Zustand von gesättigtem UO_2-Brennstoffdampf im Temperaturbereich 3000 K bis 5000 K. Die Funktionen der inneren Energie $U(T)$, spezifi-schen Wärmen $C_v(T)$ und $C_p(T)$ und der Enthalpie $H^O(T)$ und $H^O(T)-H^O_O$ werden mittels statistischer Mechanik aus verfügbaren Molekül-daten bestimmt. Bei der Untersuchung des thermodynamischen Zu-stands wird auch der Plasmazustand des gesättigten UO_2-Dampfes ermittelt und sein Beitrag zu den kalorischen Zustandsgrößen des Dampfes bestimmt. Abweichend von den idealen gaskinetischen Eigenschaften des nichtionisierten UO_2-Dampfes bis etwa 5000 K stellt die ionisierte Dampfkomponente kein gaskinetisches Plasma mehr dar. Bei Temperaturen um 5000 K erreicht gesättigter UO_2-Dampf den kollektiven Plasmazustand und wird zunehmend "metallisch". Bei der Bestimmung der kalorischen Zustands-funktionen wird auch die heterogene Gleichgewichtszusammen-setzung des UO_2-Dampfes berücksichtigt – unter Verwendung der von Breitung berechneten temperaturabhängigen Dampfzusammen-setzung. Der Beitrag der thermisch angeregten Elektronenzustände der Dampfmoleküle zur spezifischen Wärme und Enthalpie wird mit einem Rydberg-Ansatz für das UO_2-Molekül berechnet.

Die sich ergebenden Enthalpiefunktionen und spezifischen Wärmen für gesättigten UO_2-Dampf und die entsprechenden Funktionen für reines UO_2-Gas werden mit Literaturdaten für gasförmiges UO_2 bei niedrigeren Temperaturen verglichen. Versuchsweise werden mittels der Clausius-Clapeyron-Gleichung auch experimentelle Enthalpie-daten von flüssigem und festem UO_2 in die Gasphase umgerechnet. Die Korrelation mißlingt, offenbar weil die Clausius-Clapeyron-Gleichung auf das chemisch-reaktive Oxidbrennstoffsystem nicht anwendbar ist.

Contents

1. Introduction

Safety analysis of fast reactors requires knowledge of the caloric and thermal equation-of-state of oxide fuel in thermodynamic liquid-vapor equilibrium at temperatures far above 3000 K. In consequence, the thermodynamic state of saturated oxide fuel vapor, its internal energy $U(T)$ and enthalpy function $H(T)$, are of particular interest. Knowledge of these thermodynamic variables of state allows to establish a caloric equation of state of the fuel vapor and also, which may be more important, to derive theoretically the required vapor pressure curve of liquid oxide fuel by means of the oxygen potential approach of Breitung which is based on the law of mass action.

Furthermore, the caloric function of state of the fuel vapor and its gas kinetic and plasma state should be known to allow better interpretation of the laser evaporation experiments recently carried out with oxide fuel /1,2,3,4/. It is the aim of these experiments to provide experimental, reliable vapor pressure curves of liquid UO_2 and (U,Pu) mixed oxide for the LMFBR safety analysis.

In the laser evaporation experiments with UO_2 the flow-off velocity of the laser generated fuel vapor jet into vacuum turned out to be supersonic /1/. This means that the thermal surface evaporation of the fuel is followed by an intense gas dynamic expansion of the vapor plume into vacuum. This gas dynamic vapor flow-off re-acts in turn on the evaporating surface and determines the evaporation conditions at the fuel surface. The expansion of the vapor jet to supersonic velocity is driven by the enthalpy of the fuel vapor which is partly converted into kinetic flow energy. The structure of the fuel vapor jet and its reaction on the evaporating fuel surface, and the effective evaporation rate actually depend on the gaseous and plasma state, and on the gas kinetic and relaxational behavior of the oxide fuel vapor.

For the reasons above, this report deals with the thermodynamic state, and with the internal energy and enthalpy function of saturated UO_2 vapor at temperatures up to 5000 K. The caloric variables of state are deduced by means of statistical mechanics from the molecular structure and from the kinetic and plasma state of UO_2 vapor at the temperatures considered here. In a subsequent report /5/, the gas kinetic relaxation and flow structure of adiabatically expanding, laser-generated UO_2 vapor jets will be treated.

2. Enthalpy and Internal Energy of   Partly Ionized UO_2 Gas

The enthalpy function of a pure UO_2 vapor, related to one UO_2 molecule, is

$$h = u + pv, \tag{1}$$

$$v = 1/n, \text{ where } n = \text{particle density} \tag{2}$$

At temperatures below 5000 K where real gas phenomena can be neglected, the ideal gas equation holds. Therefore,

$$h = u + kT \tag{3}$$

The internal energy u - with respect to zero temperature - is related to the molecular partition function Z_m and the energy of formation Δu_f of the UO_2 molecule in its ground state.

$$u = \Delta u_f + kT^2 \cdot \frac{\partial}{\partial T} (\ln Z_m) \tag{4}$$

The complete partition function of the molecule can be factored into the product of the contributions of the various degrees of freedom of the molecule, neglecting any interactions between them.

$$Z_m = Z_{trans} \cdot Z_{rot} \cdot Z_{vib} \cdot Z_{el} \tag{5}$$

$$= Z_{trans} \cdot Z_{int}$$

The indices denote: trans = translation

$$int = \text{internal excitation}$$
$$rot = \text{rotational excitation}$$
$$vib = \text{vibrational excitation}$$
$$el = \text{electronic excitation}$$

In the high temperature region considered here, oxide fuel vapor represents a plasma, as will be discussed in Chapter 4. Therefore, eq. (4) is to be modified by the contribution from the plasma state. With χ_i denoting the ionization degree, the relation holds:

$$u = (1-\chi_i) \cdot \left[\Delta u_f + kT^2 \cdot \frac{\partial}{\partial T} (\ln Z_m) \right] \tag{6}$$

$$+ \chi_i \cdot \left[\Delta u_f + E_i^{pl} + E_{coll} + kT^2 \cdot \frac{\partial}{\partial T} (\ln Z_i \cdot Z_e) \right]$$

$$\text{with } \chi_i = \frac{c_i}{c_o + c_i} \equiv \frac{c_e}{c_o + c_i}$$

$$c_o, c_i, c_e = \text{relative concentration of neutral molecules, ions, and electrons.}$$

E_i^{pl} is the actual ionization energy of the UO_2 molecule in the UO_2 vapor in its actual plasma state. $E_{coll}(T)$ represents a (negative) binding energy term which takes into account the increasingly collective plasma state of high-temperature UO_2 vapor. Z_i and Z_e are the complete partition functions of the ionized molecule and the free electron, respectively. Factoring out the translational degree of freedom of the molecules, ions, and electrons

$$Z_{trans} = \left(\frac{2\pi mkT}{h^2} \right)^{3/2} V \tag{7}$$

yields for the internal energy, related to one (neutral or ionized) molecule:

$$u = (1-\chi_i)\left[\Delta u_f + 3 \cdot \frac{kT}{2} + kT^2 \cdot \frac{\partial}{\partial T}(\ln z_m^{int})\right]$$

$$+ \chi_i\left[\Delta u_f + E_i^{pl} + E_{coll} + 6 \cdot \frac{kT}{2} + kT^2 \cdot \frac{\partial}{\partial T}(\ln z_i^{int})\right] \quad (8)$$

In order to deduce the various contributions of the internal degrees of freedom to the internal energy function $u(T)$, we first discuss the molecular structure and the gaseous and plasma state of UO_2 vapor in the temperature region up to 5000 K.

3. Molecular Data of Gaseous Uranium Oxide Molecules

The knowledge of molecular data of isolated uranium oxide molecules appears still to be rather imperfect. Experimental data have been obtainedfrom spectroscopic matrix-isolation studies on UO, UO_2, and UO_3 /6-11/. According to the investigations by Gabelnick, Reedy, and Chasanov, the UO_2 molecule is linear-shaped and consequently has no permanent dipole moment, while the UO_3 molecule is T-shaped and appears to behave as "uranyl monoxide". It is generally assumed that the uranium oxygen and the uranium-fluorine molecules have a strong polar contribution in their actual molecular bonding /12-14/.

No experimental data exist on the electronic states of the neutral or ionized uranium oxide molecules. The same lack of data holds for the uranium ions U^{2+}, U^{4+}, U^{6+}. Based on the assumption of an ionic bonding, attempts have been made to approximate the required electronic partition function of the UO_2 molecule by the partition function of the isoelectronic Th-spectrum, excluding possible contributions from the oxygen anion. This approach has been utilized by Rosenblatt and Brewer /15/ in estimating thermo- dynamic functions of metal oxide vapor species. However, it is thought by some authors that the ionic approach overestimates the electronic contribution to the free energy function /12,17/.

In Section 5.2 of the present study, a more general approach is taken to generate the electronic partition function of UO_2, which is not restricted to a molecule of ionic bond type.

In section 5.1, the internal energy contribution from the rotational and vibrational degrees of freedom is determined. The calculation is based on the above mentioned spectroscopic data /6-11/ on the fundamental vibration and rotation modes of the uranium oxide molecules.

For the determination of the plasma state of saturated UO_2 vapor the ionization energies of uranium oxide molecules and of the uranium atom must be known. Experimental data on the first ionization potentials of these species have been published by several authors /16-19/. The following figures show magnitude and scattering of published data.

U	E_i	=	5.3 --- 6.1 eV
UO			4.3 --- 5.7
UO_2			4.3 --- 5.5
UO_3			9.5 --- 11.1

The data given above represent the ionization energies of the isolated, undisturbed molecules. The effective ionization energies, however, are remarkably lower under the actual ionization conditions in saturated UO_2 vapor, as will be shown in the next chapter.

4. Gaskinetic and Plasma State, and Molecular Composition

of UO_2 Vapor up to 5000 K

4.1 Degree of ionization of a molecular gas

The ionization degree of a high-temperature vapor consisting of UO_2 molecules can, in principle, be calculated by means of the Saha equation. It appears advisable, however, to start from the law of mass action to keep in mind the assumptions on which the Saha-equation is based.

The law of mass action for the ionization reaction is

$$\frac{c_i \cdot c_e}{c_o} = \frac{z_i \cdot z_e}{z_m} . \tag{9}$$

c_i, c_e, c_o are the relative concentrations of the ions, free electrons and molecules; z_i, z_e, z_m are the corresponding complete partition functions of these particles, which can be factored into the product of translational and internal degrees of freedom:

$$z_m = z^{trans} \cdot z_m^{rot} \cdot z_m^{vib} \cdot z_m^{el}$$

$$z_i = z^{trans} \cdot z_i^{rot} \cdot z_i^{vib} \cdot z_i^{el} \tag{10}$$

$$z_e = z_e^{trans}$$

The indices denote the translational degrees of freedom, and the various internal degrees of freedom - i.e. thermal excitation of rotational, vibrational, and electronic states.

The quotient in eq. (9) of the translational partition functions of the ionized and neutral molecule

$$z_i^{trans} = z_m^{trans} = \left(\frac{2\pi mkT}{h^2} \right)^{3/2} \cdot V$$

is equal to 1 because of the equal masses m of these particles. The same holds for the vibration and rotation terms if the neutral and ionized molecule have the same structure. As mentioned above, no experimental data exist on the electronic states of the UO_2 molecule and its ion. It is reasonable, however, to assume, that also the electronic partition functions cancel in eq. (9) - except for the exponential term exp (- E_i^{pl}/kT) representing the energetic difference of the ground states of the neutral and ionized molecule. (E_i^{pl} is the ionization energy not of the isolated UO_2 molecule but of a molecule immersed in the dense UO_2 vapor under its actual plasma conditions.) The validity of the latter assumption could be proved by a more detailed discussion, applying the Rydberg orbital model (section 5.3) to both the neutral and the ionized molecule.

The partition function of the free electrons gets reduced to their translational partition function, taking into account their statistical weight of 2.

$$z_e = 2 \left(\frac{2\pi m_e \cdot kT}{h^2} \right)^{3/2} \cdot V \qquad (11)$$

Thus, we get the familiar form of the Saha equation for the ionization degree χ_i of the UO_2 vapor:

$$\chi_i^2 = \frac{c_i \cdot c_e}{c_o} \cdot \frac{1}{c_o} = \frac{n_i \cdot n_e}{n_o} \cdot \frac{1}{n_o}$$

$$= \frac{1}{n_o} \cdot 2 \left(\frac{2\pi \cdot m_e \cdot kT}{h^2} \right)^{3/2} \cdot \exp \ (-E_i^{pl}/kT) \qquad (12)$$

n = particle number density

If we use the vapor pressure p_o of the UO_2 molecules instead of the neutral molecule density n_o, we get the Saha-equation in the form

$$\chi_i = \frac{1}{\sqrt{p_o}} \cdot 2 \left(\frac{2\pi m_e}{h^2}\right)^{3/4} \cdot (kT)^{5/4} \cdot \exp(-E_i^{pl}/2kT) \qquad (13)$$

As shown below, the ionization degree χ_i of saturated UO_2 vapor up to 5000 K turns out to be $\lesssim$ 5 %. Thus, for the quantities n_o and p_o the total particle density and total pressure of the neutral and ionized molecular species can be used without causing a remarkable error.

For convencience, the equations above are also given in their numerical form.

$$\chi_i \; /\%/ \; = \; 6,95 \cdot 10^9 \cdot \sqrt{\frac{cm^{-3}}{n_o}} \cdot \left(\frac{T}{K}\right)^{3/4} \cdot \exp\left(-E_i^{pl}/2kT\right) \qquad (14)$$

$$\chi_i \; /\%/ \; = \; .083 \; \sqrt{\frac{bar}{p_o}} \cdot \left(\frac{T}{K}\right)^{5/4} \cdot \exp\left(-E_i^{pl}/2kT\right) \qquad (15)$$

4.2 Effective ionization energy of the UO_2 molecule in UO_2 vapor

Experimental data given in the literature for the ionization energy of the isolated UO_2 molecule vary between $E_i \approx$ 4.3 eV --- 5.5 eV /16-19/. The effective ionization energy of a UO_2 molecule, however, differs remarkably from the theoretical value under the conditions of the actual gas kinetic and plasma state of saturated UO_2 vapor above 3000 K. There are several effects which lower the ionization energy - partly in an additive manner /20,21/.

The strongest effect in our case is caused by cut-off of the highly excited valence electron by the nearest neighbouring molecules. It is not the plasma state of saturated fuel vapor which is respon-sible for this effect but its large molecular density above the boiling point of UO_2 corresponding to very small values of the average molecular particle distance d_o.

As has been known from plasma kinetics, it is reasonable to assume nearly hydrogenic electronic wave functions in order to calculate this effect /21/ because the highly excited valence electron is at considerable distance of the UO_2 core and, therefore, fills a Rydberg-like orbital. The cut-off orbital is defined by the condition that the Rydberg orbital semimajor axis

$$a_n = \frac{e_o^2}{2E_{bind}} = \frac{e_o^2}{2Ry/(n-\delta)^2} = (n-\delta)^2 \cdot r_o \qquad (16)$$

e_o = electron charge

Ry = Rydberg energy = 13.6 eV

n = true orbital quantum number

δ = quantum defect constant

r_o = Bohr-radius = .53 $\overset{o}{R}$

equals $d_o/2$. The details of the Rydberg molecular model are discussed in Section 5.2. With the δ-value given there and the typical d_o values of UO_2 vapor shown in Table 3 we can immediately calculate from eqs.(17) and (18) the cut-off orbital quantum number n_{max} and the effective decrease ΔE_i of the ionization energy.

$$n_{max} = \sqrt{\frac{a_{max}}{r_o}} + \delta = \sqrt{\frac{d_o}{2r_o}} + \delta \qquad (17)$$

$$\Delta E_i = - \frac{Ry}{(n_{max}-\delta)^2} = - Ry \cdot 2r_o/d_o \qquad (18)$$

Table 1 gives the numerical results for UO_2 vapor at 5 typical temperatures from the UO_2 melting point at $\sim$ 3140 K up to 5000 K.

T	3130	3600	4000	4400	5000 K
p_o	.075	1	5	20	100 bar
d_o	111	49	30	19	12 Å
n_{max}	14.7	11.1	9.6	8.6	7.6
ΔE_i	.13	.29	.48	.76	1.2 eV

Table 1 Reduction of UO_2 ionization energy by nearest
neighbouring molecules

The Debye screening theory usually applicable to derive ΔE_i in a
kinetic plasma /20,22/ should not be applied to the UO_2 vapor
plasma because of its collective plasma state (see section 4.4).

In addition to the 'nearest neighbour effect', the ionization
energy is lowered by the action of the free electrons. Valence
electrons in continuous-like highly excited states with binding
energies $E_{bind} \lesssim kT_e$ are easily stripped off by the electron
gas and therefore must be considered to be free /22,23/. This
means, that the ionization energy is reduced additionally by
$\Delta E_i = - kT$.

Taking into account these two dominating effects, we shall use
the effective ionization energy values E_i^{pl} given in Table 2 for
the calculation of the plasma state of UO_2 vapor.

T	3130	3600	4000	4400	5000 K
kT	.270	.310	.345	.379	.431 eV
E_i^{pl}	5	4.7	4.5	4.2	3.7 eV per ion
	115.1	108.3	103.7	96.8	85.3 kcal/mole of ions

Table 2 Effective ionization energy of UO_2 in UO_2 vapor

4.3 Determination of the plasma state of UO_2 vapor

The plasma state of UO_2 vapor at temperatures between 3100 K
and 5000 K is quantitatively summarized in Table 3. It describes
the plasma state of oxide fuel vapor consisting of UO_2 or
'UO_2-like' molecules, ions and free elctrons at the temperature
T and total vapor pressure p given in the two first columns.

The numerical values are calculated from the following relation-
ships:

$$\text{particle density} \quad n_{tot} = p/kT = 7.24 \; 10^{21} \; cm^{-3} \cdot p[bar] \; /T[K]$$
$$= 7.11 \; 10^{21} \; cm^{-3} \cdot p[at] \; /T[K] \tag{19}$$

$$\text{average particle distance} \quad d_o = \left(\frac{4\pi}{3} \cdot n_{tot}\right)^{-1/3} = .620 (n_{tot})^{-1/3} \tag{20}$$

$$\text{ionization degree} \quad \chi_i = \frac{1}{\sqrt{p_{tot}}} \cdot 2 \cdot \left(\frac{2\pi m_c}{h^2}\right)^{3/4} \cdot (kT)^{5/4} \cdot \exp(-E_i^{pl}/2kT) \tag{13}$$

$$= .083 \; \% \cdot \frac{(T/K)^{5/4}}{\sqrt{p_{tot}/bar}} \cdot \exp\left(- \frac{5802 \cdot E_i^{pl}/eV}{T/K}\right) \tag{15}$$

$$\text{ion or electron density} \quad n_q = \chi_i \cdot n_{tot} \tag{21}$$

$$\text{mean ion or electron distance} \quad d_q = \left(\frac{4\pi}{3} \cdot n_q\right)^{-1/3} = .620 \; (n_q)^{-1/3} \tag{22}$$

$$\text{Debye shielding length} \quad l_D = \sqrt{\frac{\varepsilon_o}{c_o^2} \cdot \frac{kT}{n_q(Z+1)}} = 6.90 \; cm \cdot \sqrt{\frac{T/K}{2 \cdot n_q/cm^{-3}}} \tag{23}$$

Table 3 Numerical values describing the gas kinetic and plasma state of UO_2 vapor between 3100 K and 5000 K, calculated from eqs. (19) to (31)

T/K kT/eV	p bar	n_{tot} cm^{-3}	d_o Å	χ_i %	n_q cm^{-3}	d_q Å	l_D Å	l_L Å	λ_e Å	N_D	q_{LD}	λ_{PL} μm	E_i^{pl} eV	v liter/mole	A	ρ mg/cm^3
3130 .270	.075	1.74 E17	111	.67	1.16 E15	590	800	53	24	1	.1	1000	5.0	3470	a) 270 b) 269 c) 267	.08
3600 .310	1	1.97 ·E18	49	1.2	2.36 ·E16	210	190	46	22	~.3	.3	220	4.7	306	a) 270 b) 269 c) 269	.88 .88 ·87
4000 .345	5	8.89 ·E18	30	1.8	1.60 ·E17	110	77	42	21	~.07	.6	80	4.5	68	a) 270 b) 268 c) 263	3.97 3.94 3.86
4400 .379	20	3.23 ·E19	19	2.7	.872 ·E18	1oo	35	38	20	~-04	1.1	36	4.2	18.9	a) 270 b) 266 c) 259	143 14.0 13.7
5000 .431	100	1.45 ·E20	12	~5	7.2 ·E18	30	13	33	19	~.07	2.5	12	3.7	4.15	a) 270 b) 262 c) 250	65 63 60

Landau length $\quad l_L = \dfrac{1}{4\pi\epsilon_o} \cdot \dfrac{e_o^2}{kT} = 1.670 \quad 10^{-3} \; cm/T[K]$ (24)

$$= 1.439 \quad 10^{-7} \; cm/T[eV]$$

de Broglie wavelength of the free electrons $\quad \lambda_e = \dfrac{h}{\sqrt{2m_e E_e}} = \dfrac{12.3 \; Å}{\sqrt{kT/eV}}$ (25)

charged particle number in a Debye sphere $\quad N_D = n_q \cdot l_D^3$ (26)

parameter of plasma correlation $\quad q_{LD} = l_L/l_D$ (27)

plasma cut-off wavelength $\quad \lambda_{Pl} = c_o/\nu_{Pl} = 2\pi c_o \sqrt{\dfrac{\epsilon_o}{l_o^2} \cdot \dfrac{m_e}{n_q}}$ (28)

$$= \dfrac{c_o}{8979 \; s^{-1} \cdot \sqrt{n_q/cm^{-3}}} = \dfrac{3.341 \cdot 10^{10} \mu m}{\sqrt{n_q/cm^{-3}}}$$

effective ionization energy $\bar{E}_i^{Pl}$ $\qquad$ see Section 4.2

molar volume $\quad V = L/n_{tot} = 6.023 \; 10^{23}/n_{tot}$ (29)

average molecular weight
a) $\bar{A} = 2.70$ assuming uniform molecular vapor composition (UO_2)

b) $\bar{A}$ calculated for equilibrium vapor composition (UO_2, UO_3, UO, O)

c) $\bar{A}$ calculated as b) but incl. the electron gas of the ionized vapor

(30)

mass density of
the vapor

$$\rho = \bar{A} \cdot p/RT = n_{tot} \cdot \bar{A}/ 6.02 \ 10^{23} \qquad (31)$$

4.4 Discussion of the gaseous and plasma state of UO_2 vapor

Oxide fuel vapor in the temperature range from the boiling point
up to 5000 K represents a dense gaseous system. As Table 3 shows,
the mean molecular distance d_o is very small ($d_o \gtrless 10$ Å) because
of the high vapor pressure ranging between some 1 and 100 bar.
The vapor pressure data $p(T)$ of liquid UO_2 used in Table 3 are
based on own laser vapor pressure measurements /1,3/ and on the
thermodynamic calculations and theoretical evaluation of the
UO_2 vapor curve published by W. Breitung /24-26/.

From the gas kinetic point of view, saturated UO_2 vapor behaves
up to 5000 K as a perfect gas in spite of its high density. This
may be seen from an estimation of the van-der-Waals constants
of UO_2 vapor /27/.

van-der-Waals equation-of-state $(p + a/v^2) (V-b) = RT$

$$p = \text{total pressure}$$
$$= \text{kinetic pressure } p_{kin} + \text{internal pressure } p_{int}$$
$$V = \text{molar volume}$$
$$-a/v^2 = \text{(attractive) internal pressure } p_{int}$$
$$= - .42 \ (RT_c)^2/p_c \cdot v^2$$
$$= - 3.36 \ b \ (RT_c)/v^2$$
$$b = \text{'forbidden volume'}$$
$$= .125 \ (RT_c)/p_c$$

Using theoretically estimated critical UO_2 data p_c, T_c from the
literature /28,29/ the van-der-Waals constants turn out to be

$$a = \frac{174,000 \text{ cm}^3}{v^2} \text{ bar, } b = 67 \text{ cm}^3/\text{mole}$$

with $p_c = 1450$ bar, $T_c = 9300$ K

At about 5000 K the attractive pressure term a/v^2 reaches 10 % in magnitude of the total vapor pressure p and can no more be neglected at still higher temperatures.

Now the plasma state of saturated UO_2 vapor is to be discussed. Between the melting point and 5000 K, the ionization degree χ_i varies between about 1 and 5 %. This means, that in this temperature range the partial pressure of the ions and of the electron gas related to the total vapor pressure can be neglected. As Table 3 shows, the variation of χ_i is not exponential. The actual χ_i-slope with temperature can be understood by inserting into the Saha equation (13) the exponential vapor pressure equation $p = $ const.$\cdot\exp(-\Delta H_{evap}/RT)$. Because the molar heat of evaporation ΔH_{evap} exceeds the effective ionization energy (related to 1 mole), the ionization degree χ_i should even decrease with temperature. On the other hand however, referring to Table 2, the effective ionization energy remarkably decreases with temperature, which would mean a strong increase of χ_i(T). Interference of the two competing effects leads to the actual χ_i(T)-Function.

From the plasma physical point of view, saturated UO_2 vapor at temperatures up to 5000 K represents an extremely dense plasma. As Table 3 shows, the UO_2 vapor plasma does not satisfy the double inequality (32) characterizing an ordinary kinetic plasma /30/.

$$l_L \ll d_q \ll l_D \qquad\qquad (32)$$

l_D = Debye shielding distance
d_q = mean ion or electron distance
l_L = Landau length

If the right-hand inequality $d_q \ll l_D$ would be satisfied, the Debye cloud around an ion would contain a great number of electrons, which is a condition for the weakness of correlations (i.e. Coulomb interactions) compared with the thermal motion of the particles.

Also the left-hand inequality $d_q \gg l_L$ represents a condition which would exclude strong correlation effects in the plasma for two charges at a mean distance of d_q apart. If, however, l_L is of the same order of magnitude or even larger than l_D, the collective binding energy E_{coll}^{pl} of the charged plasma particles is no more weak but of the same order of magnitude as their thermal energy. The 'correlation parameter' $q_{LD} = l_L/l_D$ represents the ratio of the (negative) plasma binding energy E_{coll} (related to one ion) and the thermal energy quantum kT /30/.

$$q_{LD} = l_L/l_D = - E_{coll}^{pl}/kT = p_{int}^{pl}/p_{kin}^{pl} \qquad (33)$$

The attractive energy term $E_{coll}^{pl}(n_q T)$ is characteristic of a collective plasma with its high density. The pressure term $p_{int}^{pl} = n_q \cdot E_{coll}^{pl}$ represents the interparticle pressure of the plasma - analogous to the internal pressure of a van-der-Waals gas.

As can be seen from Table 3, the characteristic lengths of saturated UO_2 vapor above 3600 K do not satisfy eq. (32). Hence, the UO_2 vapor plasma does not approach to the state of a perfect kinetic plasma-differentfrom the above mentioned gas kinetic behavior of the non-ionized vapor component. At temperatures around 5000 K, UO_2 vapor represents a so called classical collective plasma /30/ with in-creasingly "metallic" properties. At still higher temperatures above 5000 K, UO_2 vapor should become a degenerate plasma which could be treated only by means of quantum mechanics. This uncommon gaseous plasma state is also elucidated by the fact, that at temperatures bet-ween 4500 K and 5500 K the de Broglie wavelength λ_e of the free plasma electrons should reach the magnitude of the mean molecular distance d_o and of the ion distance d_q (Table 3). Hence, there is then no more a kinetic but a wave mechanical interaction of the electron gas with the neutral and ionized molecules in the UO_2 vapor.

In Sect. 5.3, the contribution of the plasma state to the
internal energy and enthalpy function of UO_2 vapor is deter-
mined. In spite of the unusual properties of the UO_2 vapor plasma,
the energy and enthalpy content of the plasma state can be calcu-
lated straightforward and turn out to be relatively small.

4.5 Discussion of the molecular composition of UO_2 vapor

Saturated vapor over liquid UO_2 does not only consist of UO_2
molecules but to a remarkable extent also of UO_3 and UO mole-
cules, and of monatomic O.For the temperature range far above
3000 K no experimental data exist on the composition of UO_2
vapor. However, detailed thermodynamic calculations on the
equilibrium partial pressures over liquid UO_{2-x} and (U,Pu)-
oxide up to 5000 K have been performed and published by Breitung
/24/; they are based on most recent thermodynamic input data.
From this numerical set of partial pressures for saturated
vapor over liquid UO_2 the molecular composition and the average
atomic weight of the vapor can be derived. The results are given
in Table 4 for 5 different temperature values from the melting
point at ∿ 3100 K up to 5000 K. Table 4 also includes the electron
gas partial pressure calculated in Sect. 4.3. (Consequently,
by the same amount the relative total pressure of the saturated
UO_2 vapor exceeds 100 %.) The quantity $\bar{A}$ (molecule) of the last
but one line represents the average atomic weight of the mole-
cular or atomic vapor particles only. $\bar{A}$ (plasma) is the average
atomic weight of the saturated vapor over liquid $UO_{1.97}$, including
the free plasma electrons.

The plasma state of oxide fuel vapor can not be neglected in
quantitative estimations of its critical constants, e.g., by
means of the law of rectilinear diameters (Cailletet-Mathias
law). As can be seen below (Tab.3,4), neglection of the plasma
state yields too high values for the mass density or atomic
weight, resp., of the fuel vapor at T $\gtrless$ 5000 K.

The nonuniform vapor composition specified in Table 4 underscores the fact that saturated vapor of liquid UO_2 consists of chemically reactive molecular species (i.e. UO_2, UO_3, UO, O). The total oxygen content in the vapor is higher than in the liquid phase as is shown by the O/U-ratio of the vapor. Furthermore, also the average number of oxygen bonds per vapor molecule $\bar{\nu}$ is larger than in

T	3130	3600	4000	4400	5000 K
O/U ratio	1.96	2.17	2.29	2.36	2.42
O bonds per molecule $\bar{\nu}$	1.95	2.14	2.22	2.26	2.24
rel.partial pressure					
of UO_2	83.1	74.7	65.2	59.3	54.3 %
of UO_3	6.2	19.9	29.6	34.7	37.8 %
of UO	10.4	4.4	3.1	2.9	3.0 %
of O	.2	1.0	2.0	2.9	4.3 %
of O_2	0	.02	.1	.3	.6 %
of UO_2+UO_3	89.3	94.6	94.8	94.0	92.1 %
of $\sum_1^3 UO_n$	99.7	99	97.9	96.9	95.2 %
of electrons	.7	1.2	1.8	2.7	5 %
rel.total pressure	100.7	101.2	101.8	102.7	105 %
$\bar{A}$ (vapor molecules)	268.6	268.6	267.9	266.3	262.4
$\bar{A}$ (incl.plasma state)	266.7	265.	263.2	259.3	249.9

Table 4   Vapor composition and atomic weight $\bar{A}$ of saturated vapor in thermodynamic equilibrium with liquid $UO_{1.97}$.

UO_2 - indicating oxidation reactions taking place during the evaporation process. On the other hand $\bar{v}$ is smaller than the O/U-ratio of the vapor - indicating onset of dissociative reactions with increasing temperature.

In the above evaluation of the gas kinetic and plasma state, saturated vapor of UO_2 has been treated so as to consist uniformly of 'UO_2-like' molecules. The actually nonuniform vapor composition might influence only to a small extent the numerical results on the gaseous and plasma state given in Table 3. However, the following treatment of the internal energy, specific heat, and enthalpy content of UO_2 vapor takes into account the multicomponent vapor composition.

5. Internal Energy, Specific Heat, and Enthalpy Function of

Saturated UO_2 Vapor

The internal energy function $u(T)$ of the nonuniform vapor (averaged to one vapor molecule) can be established by means of eqs. (6) and (8).

$$u(T) = u_{trans} + \sum_{j=0}^{3} c_j \left[\Delta u_{f,0} + kT^2 \cdot \frac{\partial}{\partial T} (\ln Z_m^{int}) \right]_j$$

$$+ \chi_i (u_{trans}^{electron} + E_{coll}^{pl})$$

$$+ \Sigma c_j \chi_j \left[\Delta u_{f,0} + E_i^{pl} + kT^2 \cdot \frac{\partial}{\partial T} (\ln Z_i^{int}) \right]_j \qquad (34)$$

and with sufficient accuracy

$$u(T) = 3 \cdot \frac{kT}{2} + \sum_{j=0}^{3} c_j(T) \left[\Delta u_{f,0} + u_{rot}(T) + u_{vib}(T) + u_{el}(T) \right]_j$$

$$+ \chi_i(T)(c_1 + c_2) \cdot \left[3 \cdot \frac{kT}{2} + E^{pl}_{coll}(T) + E^{pl}_i(T) \right], \quad (35)$$

Index j=0 indicates the O species

=1 ------------- UO

=2 ------------ UO_2

=3 ------------ UO_3

The required internal energy function related to one mole of saturated vapor is

$$U(T) = L \cdot u(T). \qquad (36)$$

L = Avogadro number

The enthalpy function is simply obtained by

$$h(T) = u(T) + kT$$
$$H(T) = U(T) + RT \qquad (37)$$

because of the perfect gas behaviour of oxide fuel vapor up to 5000 K.

In the following sections, the various contributions from the internal degrees of freedom and from the plasma state are determined. For the energies of formation $\Delta u_{f,0}$, the data set of Table 5 is used /31/ which is based on thermodynamic data of Pattoret et al /17/, and Schick /32/.

	UO_3	UO_2	UO	O	U	
$\Delta H^o_{fo}(g)$	-9,071	-5.036	-0.4926	+2.56	+5.079	eV
	-209±5	-116.03	-11.35	58.99	117.03	$\frac{kcal}{mole}$
$\Delta u_{fo}(g)$	-21.83	-15.24	-8.132	0	0	eV
	-503	-351.04	-187.37	0	0	$\frac{kcal}{mole}$

Table 5 Enthalpies of formation of vapor molecules at 0 K.

5.1 Internal energy of rotational and vibrational excitation

The actual number of the rotational degrees of freedom of each
vapor species follows from its molecular shape. The T-shaped
UO_2 molecule has f_{rot} = 3 fundamental rotation modes, while the
linear UO_2 and UO molecules have f_{rot} = 2 possible rotation
modes. The number of the mechanic degrees of freedom of the mole-
cular vibrations results from the relation /33/

$$f^{mech}_{vib} = \begin{pmatrix} \text{number of atoms} \\ \text{in the molecule} \end{pmatrix} \times 3 - f_{rot}. \qquad (38)$$

Because there are 2 thermal energy quanta to one mechanic vib-
ration mode, the internal energy contribution of fully excited
molecular vibrations is

$$u^{vib}_j = f^{vib}_j \cdot \frac{kT}{2} \text{ with } f^{vib} = 2 \cdot f^{mech}_{vib} \qquad (39)$$

Spectroscopic molecular data mentioned above show that the rota-
tional constants of the vapor molecules are $\lesssim$ 0.5 cm^{-1} or
$\lesssim 10^{-4}$ eV. Therefore, the rotational degrees of freedom should
be fully excited already at room temperature (θ = kT = .026 eV).
The rotational contribution to the internal energy is then

$$u_{rot} = kT^2 \cdot \frac{\partial}{\partial T}(\ln Z_{rot}) = f_{rot} \cdot \frac{kT}{2} \text{ for } T \gtrsim 300 \text{ K.} \qquad (40)$$

Only one vibration mode (with $h\nu \lesssim 100/cm$) should be fully excited at room temperature. In the temperature region above 3000 K, however, all vibration modes can be expected to be fully excited, because $\theta \gtrsim 2 \cdot h\nu_{vib}$. So, we get the result:

$$u_{vib} = kT \text{ at } T \approx 300 \text{ K}$$

$$u_j^{vib} = f_j^{vib} \cdot kT \text{ for } T \gtrsim 3000 \text{ K}$$

(41)

Table 6 summarizes the rotational and vibrational degrees of freedom of the different molecular species.

species	f_{rot}	f_{vib}^{mech}	f_{vib}	$f_{rot} + f_{vib}$
UO_3	3	3	6	9
UO_2	2	4	8	10
UO	2	1	2	4
O	0	0	0	0

Table 6   Rotational and vibrational degrees of
freedom of vapor species

5.2 Internal energy of thermally excited electronic states

Up to now the spectrum of the electronic states of the UO_2 molecule has been   unknown. Therefore, in order to determine theoretically the energy content of the electronic excitation, it is necessary to use a reasonable model spectrum suitable for the actual molecule. As is known from molecular physics /33/, the energy spectrum of the unoccupied electronic states of a polyatomic molecule can be represented by a Rydberg series of states of the form

$$E_n = E_i - E_{bind} = E_i - \frac{Ry}{(n-\delta)^2} \qquad (42)$$

n = true principal quantum number of the Rydberg orbit

δ = average quantum defect constant, caused by the polarization of the singly charged molecular core

Ry = Rydberg energy = 13.6 eV

In this model, the electronic ground state orbital n_o of the molecule is occupied by that valence electron which has the smallest ionization energy. This means $E_{bind}(n_o) \equiv E_i$, with E_i being the ionization energy of the isolated neutral molecule. It is not possible to determine both constants n_o and δ from the one equation

$$E_{bind}(n_o) = E_i \quad \text{or} \quad n_o - \delta = \sqrt{\frac{Ry}{E_i}}$$

But it proves to be reasonable to characterize the ground state orbital of UO_2 by n_o = 6. Then, the quantum defect constant becomes δ = 4.3.

Each unoccupied Rydberg shell must be regarded to be degenerated by $g_n = 2 n^2$. The electronic partition function of the isolated Rydberg molecule then would be

$$z_{el} = \sum_{n=6}^{\infty} 2 n^2 \cdot \exp\left[\left(\frac{Ry}{(n-\delta)} - E_i\right) / kT\right] \qquad (43)$$

In reality, this discrete energy spectrum has to be replaced by a smeared, continuous-like spectrum, because there is no energy degeneracy of the electronic Rydberg states in a strongly bound polyatomic molecule. Furthermore, the line broadening and splitting by impacts and Stark effect of a UO_2 molecule immersed in very dense and partly ionized UO_2 vapor smear the partition function which becomes

$$z_{el} = e^{-E_i/kT} \int_{n_o}^{n_{max}} \exp\left[\frac{Ry}{(n-\delta)^2}/kT\right] \cdot \left[(2n^2+2n+\tfrac{1}{3})\,dn\right]. \qquad (44)$$

The last bracket in the integral represents the number of the no more degenerated electronic states in the interval n...n+dn.

For the internal energy contained in the thermally excited electronic states we get the expression:

$$u_{el}(T) = kT^2 \frac{\partial}{\partial T}(\ln z_{el}) \qquad (45)$$

$$= \frac{1}{z_{el}} \cdot e^{-E_i/kT} \int_{n_o}^{n_{max}}\left[E_i - \frac{Ry}{(n-\delta)^2}\right] \cdot \exp\left[\frac{Ry/kT}{(n-\delta)^2}\right](2n^2+2n+\tfrac{1}{3})\,dn$$

As already discussed in Section 4.2, the partition function of the valence electron has to be cut at a certain cut-off value n_{max} determined by the condition:

max. orbital radius = 1/2 · molecular distance d_o $\qquad (46)$

$$\text{or} \quad n_{max} = \sqrt{\frac{d_o}{2r_o}} + \delta$$

$$r_o = \text{Bohr radius} = .53 \,\overset{o}{A}$$

An analytical integration of the expressions (44), (45) is not possible. Table 7 gives the numerical values of u_{el} for 5 typical temperatures from the UO_2 melting point up to 5000 K. The input data are entered too. The f-number

$$f_{el} = u_{el}/\frac{kT}{2} \qquad (47)$$

shows the relative contribution of the elctronic excitation to the specific heat or internal energy of the UO_2 molecule.

T	3130	3600	4000	4400	5000 K
θ	.270	.310	.345	.379	.431 eV
n_{max}	15	12	10	9	8
u_{el}	.26	.339	.392	.442	.519 eV
f_{el}	2.06	2.19	2.27	2.33	2.41
with E_i = 5.5 eV, n_o = 6, δ = 4.428					

Table 7   Internal energy contribution u_{el} of electronic excitation and corresponding f-number for UO_2-like molecules.

It might be interesting to compare the results of this approach with those of a Brewer-Rosenblatt approach calculated by Fischer et al /4/ for the UO_2 molecule in which a constant electronic level density with constant statistic weight was assumed. The latter approach would yield 2.1 to 2.5 thermal degrees of freedom for the electronic states at temperatures between 3100 K and 5000 K. These values are slightly higher (by some 4 to 11 %) than the results of the approach presented here.

In the energy balance for saturated UO_2 vapor in Sect. 5.3, the above given specific heat $C_v = f_{el} \cdot RT/2$ of the electronic excitation of the UO_2 molecule is also assigned to the other uranium oxide species of the vapor.

5.3 Internal energy of the plasma state

The additional energy contribution from the plasma state is described by the last bracket term in eq. (35).

$$u_{pl}(T) = f_{pl} \cdot kT/2$$

$$= \chi_i(T) \cdot (c_1 + c_2) \cdot \left[3\frac{kT}{2} + E^{pl}_{coll}(T) + E^{pl}(T) \right] \quad (48)$$

Thermal ionization of the electronically stable UO_3 molecules is ignored in this energy balance. The average ionization degree χ_i, the concentrations c_j of UO_2 and UO molecules, and the mean ionization energy (i.e. $E^{pl}_i + kT$) can be taken from Table 3 and Table 4. The collective binding term $E^{pl}_{coll}(T)$ is negative and follows from eq. (33).

Table 8 shows numerically the resulting f-number and the internal energy content of the thermal degrees of freedom of the plasma state, calculated for both saturated UO_2 vapor of equilibrium composition and pure UO_2 vapor of the same pressure. The contribution from the plasma state turns out to be only 1 to 5 % of the total specific heat $C_v = f \cdot R/2$ (see Tab. 9).

T	3130	3600	4000	4400	5000 K	T
f_{pl}(sat.vapor)	.25	.31	.34	.39	.43	$U_{pl}/\frac{cal}{mole \cdot K}$
$f_{pl}(UO_2$ gas)	.27	.39	.50	.62	.76	$U_{pl}/\frac{cal}{mole \cdot K}$

Table 8   Internal energy contribution from the plasma
state of UO_2 vapor

5.4 Total specific heat of UO_2 vapor between 3000 and 5000 K

Insertion of the results of section 5.1 to 5.4 into eq. (35)-
non-observing the temperature-independent additive terms
$(\Delta u_{f,o})_j$ - and derivation at constant vapor composition yields
the specific heat of saturated UO_2 vapor, and - setting $c_2 = 1$,
$c_0 = c_1 = c_3 = 0$ - the specific heat of pure UO_2 vapor. As
Table 9 and Fig.1 show, saturated UO_2 vapor of equilibrium
composition has a specific heat which is higher by 3 to 11%
than that of uniform UO_2 gas.

T	3140	3600	4000	4400	5000	
$C_v / \dfrac{cal}{K \cdot mole}$	18.6	15.8	15.6	15.4	15.1	UO_2 vapor of equil.compos.
$C_v / \dfrac{cal}{K \cdot mole}$	16.8	14.3	14.5	14.6	14.6	pure UO_2 gas

Table 9

5.5 Internal energy and enthalpy function of UO_2 vapor up to 5000 K

The functions of internal energy and enthalpy of UO_2 vapor are
summarized numerically and graphically in Table 10 and Fig. 2.
The absolute enthalpy function $H^o(T)$ is obtained from eqs. (35)
to (37). Zero reference state is **related to the gaseous elements** U
and O at 0K. The relative energy and enthalpy functions are obtained
from the equations above by ignoring the additive terms of
the energies of formation $(\Delta u_{f,o})_j$. (The vapor composition is
assumed to be the same at temperature T and reference temperature
T_o.)

T		3130	3600	4000	4400	5000 K	
U_T-U_{300}	a)	1.856	2.214	2.471	2.717	3.061	eV
	b)	1.961	2.299	2.631	2.941	3.394	
U_T-U_{300}	a)	42.76	51.02	56.92	62.61	70.54	kcal/mole
	b)	45.18	52.91	60.92	67.77	78.20	
$H_T^O-H_{300}^O$	a)	48.38	57.58	64.28	70.75	79.87	kcal/mole
	b)	50.80	60.12	67.97	75.92	87.54	
$H_T^O-H_O^O$	a)	51.0	60.30	67.02	73.50	82.61	kcal/mole
	b)	53.48	62.80	70.65	78.60	90.22	
$H^O(T)$	a)	-291.31	-310.27	-316.69	-314.78	-303.90	kcal/mole
	b)	-297.52	-288.2	-280.35	-272.40	-260.78	

Table 10 Internal energy and enthalpy of
a) saturated UO_2 of equilibrium composition
b) UO_2 gas consisting of UO_2 molecules only.

① sat. vapor over liquid UO_2
② UO_2 gas of same pressure as ①
③ UO_2 gas. Ref. / 32 /
④ UO_2 gas. Ref. / 17 /
⑤ UO_2 gas. Ref. / 12 /
⑥ UO_2 vapor. Ref. / 4 /
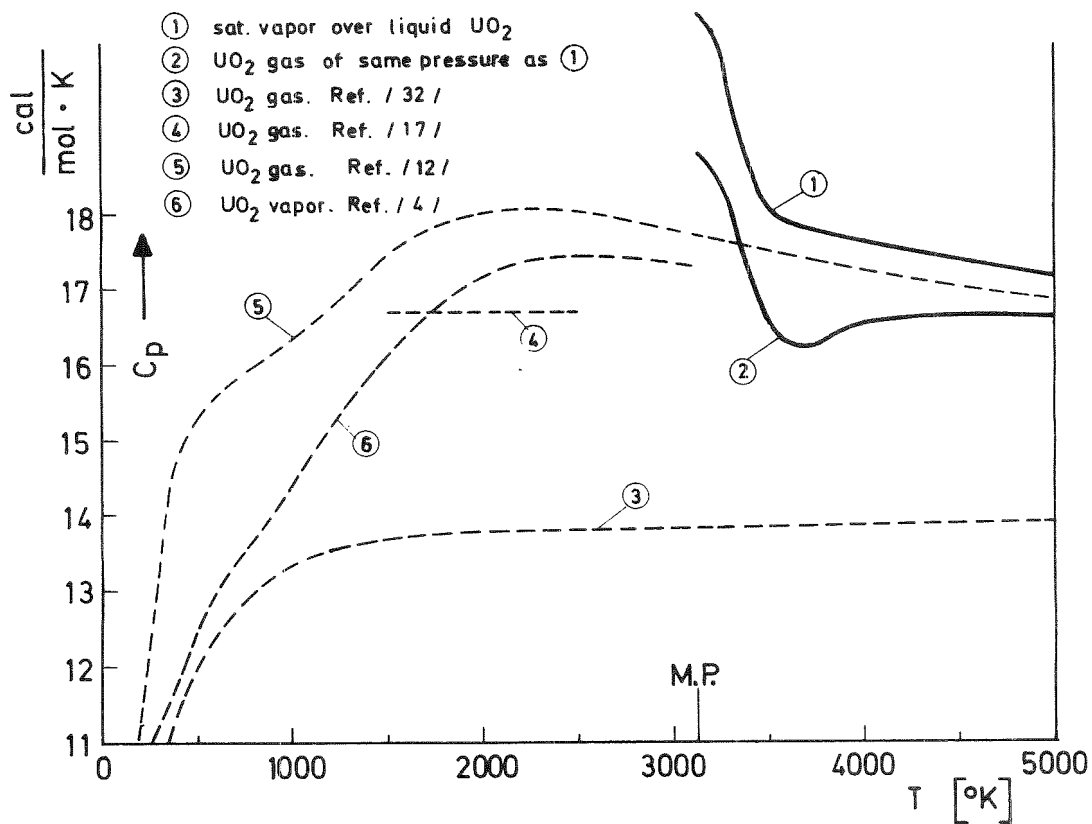
Fig. 1 Specific heat $C_p(T)$ of
1) saturated UO_2 vapor of equilibrium composition
2) UO_2 vapor, assuming uniform composition of UO_2 molecules
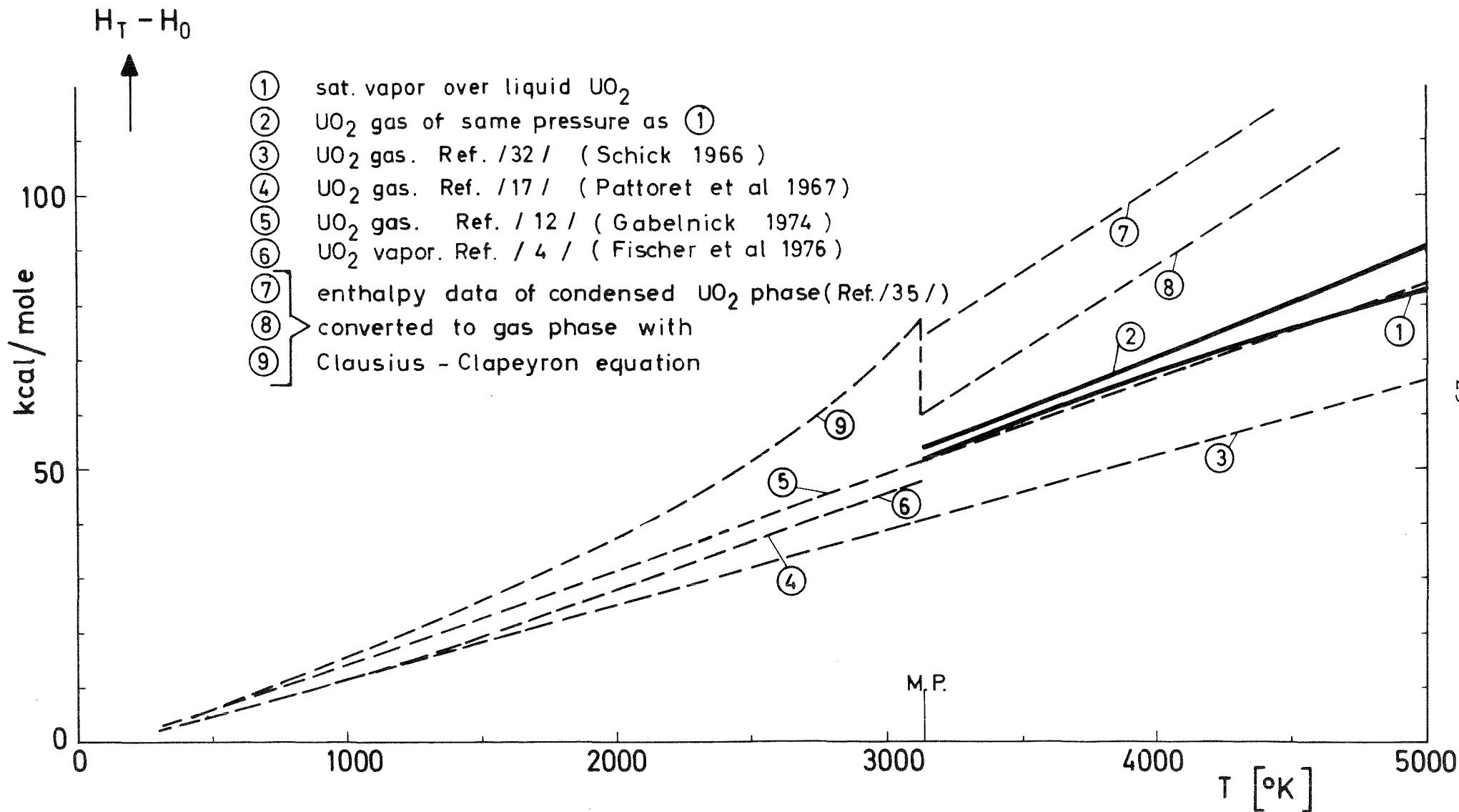
Fig. 2 Enthalpy function $H^o(T) - H^o_o$ of

1) saturated UO_2 vapor of equilibrium composition

2) pure UO_2 gas

6. Discussion of Results
_____

The determination above of the internal energy, specific heat, and enthalpy of high-temperature UO_2 vapor by means of statistical mechanics differs from previously published approaches because it comprises the dense plasma state of saturated UO_2 vapor including the thermal excitation of electronic states of the vapor molecules. In addition it has been taken into account that the equilibrium composition of uranium oxide vapor over liquid UO_2 is nonuniform and changes with temperature. For these reasons deviations of previously published thermodynamic UO_2 vapor functions from the approach presented here appear to be reasonable.

Fig.1 gives a comparison of the specific heat function $C_p(T)$ of UO_2 vapor assuming saturated equilibrium composition (curve No 1) and uniform UO_2 composition (curve No 2) with the specific heat data sets for pure UO_2 vapor of Schick/32/, Gabelnick/12/, and Fischer et al./4/, respectively. The non-monotonous slope with temperature of the new specific heat functions is primarily caused by the changes in the vapor composition and in the plasma state with temperature. The overshoot of $C_p(T)$ near the melting point (3140 K) is caused by the onset of thermal excitation of the electronic states, and of thermal ionization of the vapor molecules.

At temperatures up to 5000 K, the specific heat of UO_2 vapor contains a relatively small energy contribution from the plasma state, as is assessed in Table 8. The negative binding energy of the plasma state still diminishes its role in the energy balance of UO_2 vapor, revealing the collective vapor plasma to be some kind of stable charged particle arrangement, since energy is needed to destroy it /30,34/. On the other hand, the dense plasma state of UO_2 vapor (Sect.4.4) may significantly stamp. e.g., its optical and radiation properties and eventually influence the liquid-vapor equilibrium. (It should also be noted that a collective plasma state limits the quantitative validity of the Saha equation).

Fig. 2 gives a comparison of the enthalpy functions H(T) - H(OK) of saturated UO_2 vapor (curve No 1) and of pure UO_2 gas (curve No 2) with UO_2 enthalpy functions found in literature. The high-temperature enthalpy function of gaseous UO_2 published by Schick /32/ (curve No 3) runs clearly below the enthalpy data of this report. The same holds for the enthalpy data near the melting point given by Pattoret et al./17/ and Fischer et al./4/. The deviation between curve No 2 for pure UO_2 gas and the enthalpy data of Gabelnick /12/ (curve No5) is only 4...7%.

It might be interesting to compare, if possible, the present enthalpy data of gaseous UO_2 with enthalpy data from literature of the condensed UO_2 phases. For that purpose, the enthalpy data set of solid and liquid UO_2 recommended by Leibowitz et al. /35/ is converted tentatively to the gaseous phase by means of eq. (49).

$$H(T) - H_0\Big|_{vapor} = H(T) - H_0\Big|_{cond.} + \Delta H_{evap}(T) - \Delta H_{evap}(0) \tag{49}$$

This approach simply follows from the Clausius-Clapeyron equation

$$\frac{dp}{dT} = \frac{H_{vap} - H_{cond}}{(V_{vap} - V_{cond})T} \tag{50}$$

Enthalpy curve No 7 (Fig. 2) represents the enthalpy conversion for the UO_2 vapor component with $\Delta H_{evap}(T) = 124.62$ kcal/mole and $\Delta H_{evap}(0) = 143.5$ kcal/mole derived from Breitung's oxygen potential approach for UO_2 /24/. Curve No 8 is based on $\Delta H_{evap}(T) = 111.6$ kcal/mole and $\Delta H_{evap}(0) = 143.2$ kcal/mole obtained from the ANL data set /35/. Curve No 9, which would represent the enthalpy of saturated UO_2 vapor over solid UO_2 has been normalized to H(300) - H(0) = 2.68 kcal/mole.

As Fig. 2 shows, the Clausius-Clapeyron approach would lead
to very high specific heat and enthalpy values of the vapor,
which do not appear to be realistic. The discrepancy could
be caused by the application of the Clausius-Clapeyron
equation /4/. This conclusion may be confirmed by considering
the absolute enthalpy function $H^O(T)$ of saturated UO_2 vapor
(Table 10). Its slope is nonmonotonous because of the strong
changes in vapor composition with temperature. Use of $H^O_{gas}(T)$
in eq. (50) together with the monotonous $H_{liqu.}(T)$ function
would lead to a strange-looking total vapor pressure curve of
liquid UO_2.

Actually, application of the Clausius-Clapeyron equation tacitly
assumes that the observed vapor-liquid equilibrium belongs to a
single-component, chemically inert thermodynamic system. The
oxide fuel system does not satisfy this assumption. Even restriction
to the partial system 'condensed UO_2 phase - gaseous UO_2 vapor
component' would not allow application of eq. (50), because the
partial system would not represent a closed thermodynamic system
/36/.-For the same reasons, also results obtained from the gene-
ralized Clapeyron equation for multicomponent systems /37/ should
be viewed with reservation, if applied to the vapor-liquid equili-
brium of oxide fuel systems, - e.g., the relation between azeo-
trope (i.e. congruent evaporation composition) and a vapor pressure
minimum. - Under these aspects the discrepancy of enthalpy data
in Fig. 2 seems to be cleared up.

The approach above of calculating the specific heats of the uranium
oxide vapor species can be completed by determination of the free
energy functions of the vapor species, including thermal ionization
and electronic excitation. By use of Breitung's oxygen potential
approach for the UO_2 system, this independent set of input data
for the vapor phase together with appropriate data for the con-
densed phase /24, 35/ would allow to verify the previously
published equilibrium vapor pressure curves over liquid
oxide fuel /24, 25, 26/.

7. Literature

/1/   M. Bober, H.U. Karow, K. Schretzmann
      Proc. IAEA Symp. on Thermodynamics of Nuclear
      Materials 1974
      Vienna 1975. Vol. 1, page 295

/2/   R.W. Ohse, P.G. Berrie, H.G. Bogensberger, E.A. Fischer
      ibid. Vol 1, page 307

/3/   M. Bober, W. Breitung, H.U. Karow, K. Schretzmann
      Report KFK 2366 (1976)

/4/   H.G. Bogensberger, E.A. Fischer, P.G.Berrie ,
      R.W. Ohse
      Report KFK 2272 (1976)

/5/   H.U. Karow
      Report KFK 2391 (in preparation)

/6/   H.J. Leary, E.D. Cater, H.B. Friedrich, T.A. Rooney
      Report COO-1182-34. Univ. of Jowa (1971)

/7/   S. Abramowitz, N. Acquista, K.R. Thompson
      J. Phys. Chem. 75 (1971) 2283

/8/   S. Abramowitz, N. Acquista
      J. Phys. Chem. 76 (1972) 648

/9/   D.H.W. Carstens, D.M. Gruen, J.F. Kozlowski
      High Temp. Science 4 (1972) 436

/10/   S.D. Gabelnick, G.T. Reedy, M.G. Chasanov
      Chem. Phys. Lett. 19 (1973) 90

/11/   S.D. Gabelnick, G.T. Reedy, M.G. Chasanov
      J. Chem. Phys. 58 (1973) 4468
/12/   S.D. Gabelnick, Report ANL-8120 (1974).
      S.D. Gabelnick. Private communication

/13/   C. Keller. Private communication
/14/   E. Jakob (MAN Munich). Private communication
      W. Bacher (Karlsruhe Nucl. Res. Center).
      Private communication

/15/   L. Brewer, G.M. Rosenblatt, Chem. Rev. 61 (1961) 257
      L. Brewer, G.M. Rosenblatt, Adv. High Temp. Chem. 2 (1969) 1
      L. Brewer, J. Opt. Soc. Amer. 61 (1971) 1101

/16/   J.B. Mann,
      J. Phys. Chem. 40 (1964) 1632

/17/ A. Pattoret, J. Drowart, S. Smoes
Proc. IAEA Symp. on Thermodynamics of Nuclear
Materials, 1967. Page 613.
Vienna 1968

/18/ K.G. Heumann
Int. J. Mass Spectrom. Ion Phys. 9 (1972) 315

/19/ E.G. Rauh, R.J. Ackermann
J. Chem. Phys. 60 (1974) 1396

/20/ H.R. Griem, Plasma Spectroscopy, New York 1964

/21/ G.V. Marr, Plasma Spectroscopy, Amsterdam 1968

/22/ H.U. Karow
Report KFK 1870 (1973)

/23/ Ya. B. Zeldovich, Yu. P. Raizer
Physics of Shock Waves and High Temperature
Hydrodynamic Phenomena
(Eds. W.D. Hayes, R.F. Probstein) New York 1966

/24/ W. Breitung
Report KFK 2091 (1975)

/25/ M. Bober, W. Breitung, H.U. Karow, K. Schretzmann
J. Nucl. Mater. 60 (1976) 20

/26/ W. Breitung
Report KFK 2240 (1976)

/27/ E.A. Moelwyn-Hughes
Physical Chemistry, Oxford 1964

/28/ M.J. Gillan
Proc. IAEA Symp. on Thermodynamics of Nuclear
Materials 1974
Vienna 1975

/29/ D. Miller
Report ANL 7120 (1965)

/30/ J.L. Delcroix
Physique des Plasmas, Paris 1963

/31/ W. Breitung, Private communication

/32/ H.L. Schick
Thermodynamics of Certain Refractory Compounds
New York 1966

/33/ G. Herzberg
Molecular Spectra and Molecular Structure, Vol. III.
Electronic Spectra and Electronic Structure of
Polyatomic Molecules, New York 1966

/34/ V.S. Vorobev, A.L. Khomkin
Teplofizika Vysokikh Temperatur 14 (1976) 204

/3 5/ L. Leibowitz et al.
Report ANL-CEN-RSD-76-1 (1976)

/36/ E. Hala, J. Pick, V. Fried, O. Vilim
Vapor-Liquid Equilibrium, Oxford 1967

/37/ R. Gilmont
Vapor-Liquid Equilibrium.
Enc. Chemical Technology 21 (1970) 196.
(Edts. Kirk -Othmer)